applied sciences

MDPI

Article

Investigation of the Influence of Liquid Motion in a Flow-Based System on an Enzyme Aggregation State with an Atomic Force Microscopy Sensor: The Effect of Water Flow

Yuri D. Ivanov [1,*], Tatyana O. Pleshakova [1], Ivan D. Shumov [1], Andrey F. Kozlov [1], Tatyana S. Romanova [1], Anastasia A. Valueva [1], Vadim Yu. Tatur [2], Igor N. Stepanov [2] and Vadim S. Ziborov [1]

[1] Institute of Biomedical Chemistry, 10, Pogodinskaya St., 119121 Moscow, Russia; t.pleshakova1@gmail.com (T.O.P.); shum230988@mail.ru (I.D.S.); afkozlow@mail.ru (A.F.K.); romtatyana@mail.ru (T.S.R.); varuevavarueva@gmail.com (A.A.V.); ziborov.vs@yandex.ru (V.S.Z.)

[2] Foundation of Perspective Technologies and Novations, 115682 Moscow, Russia; v_tatur@mail.ru (V.Y.T.); stepanovigorn@gmail.com (I.N.S.)

* Correspondence: yurii.ivanov.nata@gmail.com

Received: 26 May 2020; Accepted: 26 June 2020; Published: 30 June 2020

Featured Application: The influence of an electromagnetic field, which is induced upon the motion of water through polymeric communication pipes, on the aggregation state of proteins, should be taken into account in the development of novel highly sensitive biosensor systems intended for the early diagnosis of diseases. This effect observed herein should also be considered in the development of specified models of hemodynamics.

Abstract: The influence of liquid motion in flow-based systems on the aggregation state of an enzyme and on its enzymatic activity was studied, with horseradish peroxidase (HRP) as an example. Our experiments were carried out in a setup modeling the flow section of the biosensor communication with a measuring cell containing a protein solution. Studies were conducted for a biosensor measuring cell located along the axis of a spiral-moving liquid flow. The aggregation state of the protein was determined with an atomic force microscopy-based sensor (AFM sensor). It has been demonstrated that upon flowing of water through silicone biosensor communications, an increased aggregation of HRP protein was observed, but, at the same time, its enzymatic activity did not change. Our results obtained herein are useful in the development of models describing the influence of liquid flow in biosensor communications on the properties of enzymes and other proteins. This is particularly important for the development of serologic protein biosensors, which are beginning to be used for the early diagnosis of oncological diseases (such as brain cancer, prostate cancer, breast cancer etc.). The results obtained herein should also be taken into account when considering possible changes in hemodynamics due to increased protein aggregation.

Keywords: horseradish peroxidase; atomic force microscopy sensor; protein aggregation

1. Introduction

In biosensor systems, spiral-coiled communications with a flowing aqueous medium are often used for thermal stabilization. Such communications are employed both in miniaturized biosensor systems and in large bioreactors [1]. Upon the flowing of water through spiral-wound

communications, triboelectric effects occur [2–6]; the occurrence of such effects leads to the generation of an electric current. In turn, the motion of electric charges (i.e., the electric current) is known to induce electromagnetic fields. Despite these fields being weak, they nevertheless can influence biological objects. As is known, weak electromagnetic radiation, whose power is in the range of ~10^{-4} W, has an influence on human body (though this influence is weak)—so-called non-thermal effects [7,8]. Studying these effects is of great importance, since weak radiation is beginning to be used in medicine for disease treatment. For instance, pilot research is being undertaken to study the therapeutic effect of electromagnetic radiation of non-thermal power in cancer [7]. At the same time, the influence of weak electromagnetic radiation on enzyme systems is still insufficiently studied. So, a number of studies have concerned the aggregation state of proteins in biosensor systems [9,10], but the influence of inductive electromagnetic fields was not considered. On the other hand, it was demonstrated that a triboelectric effect appears upon flowing of water in polymeric pipes, which leads to a generation of charge [2–6]; accordingly, an electromagnetic field is induced. In modern biosensors, polymeric materials are widely used in fluidic communications, in thermostabilization systems etc.

Recent experimental studies showed that the triboelectric effect is observed not only for pure (deionized or distilled) water, but also for tap water [11–13] and even for 0.6 M NaCl and seawater [11,12], whose resistivity is low.

At that, obviously, biosensors are fabricated in the form of compact devices, to save materials, working space etc. Since an electric field is induced upon the flowing of a liquid through communication components, the influence of this field can spread beyond these components. Accordingly, it is of interest to find out the relationship between the process of the flowing of a liquid sample and the properties of the sample located, for instance, in the measuring cell.

Thus, in our present study, typical conditions occurring in a biosensor or in a bioreactor have been modeled, and the influence of flowing of water through spiral communications of a biosensor on the properties of a protein, with an example of a well-studied protein—horseradish peroxidase (HRP) enzyme—has been investigated. HRP pertains to heme-containing enzymes [14]. These enzymes play an important role in various metabolic processes in human [15]. Moreover, HRP is often employed in biosensor analysis as an enzymatic tag [16,17]. These are the reasons why this protein has been chosen as a model object for our study. In our present research, HRP has been employed as an object of study, since this protein is a well characterized enzyme often used as a model in studies of a wide class of peroxidases. The study of peroxidases is of great interest due to the fact that these enzymes are well represented in plant and animal tissues [18] and play an important functional role in the organism. Peroxidase catalyzes the oxidation of a broad spectrum of organic and inorganic compounds by hydrogen peroxide [19]. In particular, one should point out an important role of myeloperoxidase, which participates in atherogenesis in humans [20]. The molecular weight of HRP heme-containing glycoprotein is 40 to 44 kDa [21,22]. It is known that many enzymes, including horseradish peroxidase [23], form aggregates. It was demonstrated that a change in the aggregation state of HRP is observed upon the influence of electromagnetic fields with 100 Hz to 100 kHz frequencies. So, aggregation of this protein was observed in alternating magnetic field with 40 kHz frequency at various intensities from 510 to 1230 kA/m [24]. Neither a constant magnetic field nor alternating electric field with the frequency within the range from 100 Hz to 100 kHz caused any change in the aggregation state of HRP; however, a significant aggregation was observed in the case of the combination of these fields [25].

In this way, the aggregation state of HRP biomolecules can be used as an indicator of the effect of electromagnetic fields on biological molecules. A change in the aggregation state of an enzyme due to an external physicochemical impact—such as electromagnetic, thermal, and chemical—characterizes a change in its spatial structure. The latter can lead to changes in its functional properties and, as a consequence, to a pathological state of the whole organism.

To study the effect of the electromagnetic field on HRP aggregation, an atomic force microscopy-based sensor (AFM sensor) has been employed. The use of the AFM-based approach for studying the effect of weak knotted electromagnetic fields on the aggregation state of HRP was demonstrated in

our recent study [26]. In this way, one more reason why this protein has been chosen as a model object for our present study is the fact that the aggregation state of HRP is rather sensitive to the influence of weak electromagnetic fields. The importance of data obtained upon monitoring protein aggregation consists of the possibility of the registration of minor effects, as every (even insignificant) change in protein structure can affect the aggregation state of the macromolecules. At that, changes in the structure are pronounced as an integral effect, which is connected with both the interaction between proteins in their aggregates and the protein–surface interactions. To study protein aggregation, light scattering-based methods such as dynamic light scattering (DLS) and multi-angle light scattering (MALS) are commonly employed. It is to be noted that these methods are used for the determination of protein aggregation in solution. In our present study, we employed AFM to determine the possibility of protein aggregation on the surface, since in such a case it is possible to observe additional effects of interaction of the protein with the AFM substrate surface. Due to such effects, the results obtained by DLS can differ from those obtained by AFM. In addition, it should be noted that, to ensure the intensity of the scattered light is not lower than the DLS device sensitivity threshold, DLS experiments often require much higher protein concentrations than those used in AFM experiments [27]. At the same time, concentration effects can significantly influence the HRP aggregation state [23,28]. This is another reason why the results obtained by AFM and by DLS can differ. In the framework of the present study, our task consisted of the revelation of changes in the protein's properties under the influence of electromagnetic field induced by the water flow at the single-molecule level. Due to the above-listed factors, these changes can be indistinguishable while using DLS; these changes, however, manifest themselves upon using AFM, when the signal from individual macromolecules is detected [29,30]. AFM allows one to visualize individual enzyme molecules [29,30], which is important for single molecule enzymology. To monitor the aggregation state of HRP in solution before and after its exposure to the field, atomic force microscopy visualization of HRP macromolecules, adsorbed from this solution onto atomically smooth substrate surface, was performed. In parallel, the enzymatic activity of HRP was monitored by conventional spectrophotometry. In our research, these two methods were employed together, as it was assumed that weak electromagnetic field can influence the properties of HRP as discussed above. However, in cases when this change does not affect either the active site or chromophoic groups of the enzyme, it is difficult to reveal such changes by measuring the kinetic parameters of the enzyme reaction.

Herein, we modeled the measuring cell of a biosensor (or a bioreactor vessel) using a standard polypropylene tube filled with HRP solution, while the polymeric communication was modeled with a silicon pipe, spiral-wound onto a glass cylinder to form a coil, through which tap water was pumped (see Figure 1). Such a geometry is often used in thermostabilization of biosensors' elements, including measuring cells, and in a number of other cases. The cell was placed over the spiral-wound pipe parallel to the coil axis (over the coil) (Figure 1). Our AFM data indicated that in the case when the cell, containing HRP solution, was placed over the coil, an increase in the HRP protein structures (that is, HRP aggregation) was observed. At that, according to the spectrophotometric data, enzymatic activity of HRP did not change.

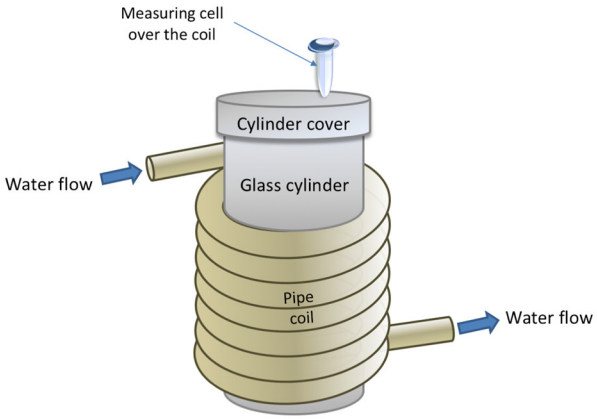

Figure 1. Schematic representation of the experimental setup employed for studying the effect of liquid flow on the properties of a protein. The measuring cell with the enzyme solution was placed over the coil; "water flow" marks indicate start and end section of the silicone pipe, which was spiral-wound onto a glass cylinder to form a coil; water was pumped through the coiled pipe.

Moreover, to study the inductive field (induced by the motion of water) along the communication axis, kinetic studies were conducted to measure the action of this field on a metal disk suspended on a cobweb thread along the axis of this communication. This system modeled highly sensitive torsion balance, commonly used in physics to study the induced fields by monitoring the torsion of a disc. It was obtained that the inductive field influences the position of the disc, making it spin. This motion was recorded on a video.

The results obtained herein should be taken into account in the analysis of the structure of proteins and their complexes studied using biosensors, in the development of serological diagnostics based on protein markers of diseases requiring early diagnosis, such as brain cancer, prostate cancer, etc. These data can also be of use in the study of hemodynamics in the human body.

2. Materials and Methods

2.1. Chemicals and Protein

Peroxidase from horseradish (HRP-C; Cat.# P6782) was obtained from Sigma (St. Louis, MO, USA). 2,2′-azino-bis(3-ethylbenzothiazoline-6-sulfonate) (ABTS) was purchased from Sigma. Disodium hydrogen orthophosphate (Na_2HPO_4), citric acid and hydrogen peroxide (H_2O_2) were purchased from Reakhim (Moscow, Russia). All solutions were prepared using deionized ultrapure water (with 18.2 MΩ×cm resistivity) obtained with a Simplicity UV system (Millipore, Molsheim, France).

2.2. Experimental Setup

Experimental setup is schematically shown in Figure 1. The model of a biosensor communication imitated a flow section and a measuring cell. The flow section was represented by a polymeric pipe (o.d. = 10 mm) spiral-wound (13 turns) onto a glass cylinder (d = 170 mm), so that the coil length was 130 mm.

In the experiments, 10^{-7} M aqueous solution of HRP was used. This solution was obtained by sequential tenfold dilution of 10^{-5} M stock solution, which was prepared by dissolving 0.15 mg of an initial HRP preparation in 0.375 ml of ultrapure water. A standard 1.7-ml Eppendorf-type polypropylene tube modeled a measuring cell, into which 1 ml of aqueous solution of HRP was placed. The cell was placed in relative to the flow section along the coil axis (see Figure 1).

In the experiments, tap water (Moscow, Russia; the water quality satisfied Russian Federation SanPin) was pumped through the coiled pipe. The experiments were carried out at room temperature (RT, 23 °C). Water was pumped with a peristaltic pump, and the pumping speed was 4 m/s. The cell containing HRP solution was placed in the position shown in Figure 1 for 40 min. After that, the solution was subjected to AFM and spectrophotometric analysis.

In the control experiments, the cell with HRP solution was placed away (at a distance of 10 m) from the experimental setup for 40 min. After that, the measurements were performed analogous to the working experiments.

To estimate the effect of the inductive field, arising from the motion of liquid, on a mechanical torsion of a disc, an aluminum disc (disc diameter 80 mm, mass 400 g) was hung on a cobweb thread to the top lid of a glass cylinder with the polymeric pipe coil. The disc was marked with tick marks to track the angle of rotation. The disc rotation upon starting the water flow through the pipe coil was recorded on a video. For this purpose, a video camera was placed on top of the cylinder and was aimed at the bottom of the cylinder, recording the disc rotation.

2.3. AFM Sensor Measurements

The AFM sensing experiments were carried out as described in our recent study [26]. Briefly, HRP was non-covalently immobilized onto the surface of bare muscovite mica sheets (SPI, USA) from 800 μL of 0.1 μM aqueous HRP solution by direct surface adsorption method [31]. The protein concentration used in AFM sensing experiments was determined by the inherent limitations of the AFM sensing technique: at higher concentrations, the investigated molecules formed continuous layers on the mica surface, thus hindering the visualization of individual objects [31].

The mica surface with adsorbed HRP molecules was visualized with an AFM-based sensor according to the previously developed technique [26]. The AFM images were recorded in tapping mode in air employing a Titanium multimode atomic force microscope (which pertains to the equipment of "Human Proteome" Core Facility of the Institute of Biomedical Chemistry, supported by Ministry of Education and Science of Russian Federation, agreement 14.621.21.0017, unique project ID RFMEFI62117X0017; NT-MDT, Zelenograd, Russia) equipped with NSG10 cantilevers ("TipsNano", Zelenograd, Russia; 47 to 150 kHz resonant frequency, 0.35 to 6.1 N/m force constant). The calibration of the microscope by height was carried out on a *TGZ1* calibration grating (NT-MDT, Russia; step height 21.4 ± 1.5 nm). The total number of imaged objects in each sample was no less than 200, and the number of frames for each sample was no less than 10. Analogously to one of our recent papers, the density of distribution of the imaged objects with height $\rho(h)$ was calculated as $\rho(h) = (N_h/N) \times 100\%$, where N_h is the number of imaged proteins with height h, and N is the total number of imaged proteins [32]. Preliminary experiments were performed with the use of protein-free ultrapure water instead of protein solution; in these experiments, no objects with >0.5 nm height were registered.

AFM sensor operation, obtaining AFM images, their treatment (flattening correction etc.) and exporting the obtained data in ASCII format were performed using the standard NOVA Px software (NT-MDT, Moscow, Zelenograd, Russia) supplied with the atomic force microscope. The number of the visualized particles in the obtained AFM images was calculated automatically using specialized AFM sensor data processing software developed in Institute of Biomedical Chemistry.

2.4. Spectrophotometric Estimation of Enzymatic Activity of HRP

HRP activity monitoring was estimated according to the technique described in detail by Sanders et al. [33] employing (ABTS) as reducing substrate. ABTS is commonly employed for the determination of HRP enzymatic activity, and the enzymatic assay reaction should be performed at pH 5.0 [34]. Briefly, the rate of change in solution absorbance at 405 nm was measured employing an Agilent 8453 UV-visible spectrophotometer (Agilent Technologies Deutschland GmbH, Waldbronn, Germany). Then, 30 μL of 10^{-7} M HRP solution was added into a 3-mL quartz cuvette (pathlength 1 cm, Agilent, USA) containing 2.96 mL of 0.3 mM ABTS solution in phosphate-citrate buffer (51 mM

Na_2HPO_4, 24 mM citric acid, pH 5.0) and stirred. In this way, the final HRP concentration in the cuvette was 10^{-9} M. Finally, 8.5 µl of 3% (w/w) H_2O_2 was added into the cuvette. Spectrum acquisition was started immediately upon the addition of H_2O_2.

3. Results

3.1. Results of AFM Sensor Measurements

Figure 2 displays typical AFM images of the mica surface with HRP biomolecules adsorbed from the working solutions and from the control solution, and corresponding cross-section profiles indicated by the lines in the images. Figure 3 displays the density functions of distribution of the imaged objects with height $\rho(h)$, plotted based on the AFM data summarized for each sample.

As seen from Figure 2a, in the control experiment, when the cell containing HRP solution was placed far away from the polymeric pipe coil, the protein adsorbs onto the mica surface in the form of compact objects with heights from 1.0 to 4.0 nm. The $\rho(h)$ plot (Figure 3, black line) indicates that the maximum number of molecules have a height of 1.6 ± 0.2 nm. The molecular weight of HRP is known to be 40 to 44 kDa [21,22]. Furthermore, other proteins with similar M_r were reported to have comparable sizes: putidaredoxin reductase, h_{max} = 1.8 nm [27], M_r = 45.6 kDa [35]; adrenodoxin reductase, h_{max} = 1.8 nm [36], M_r = 54 kDa [37]. Our data obtained herein are also in coincidence with the results obtained in our previous studies by AFM [26,28]. For these considerations, one can conclude that the objects with ~1.6-nm height, observed upon AFM scanning, can be attributed to HRP monomers.

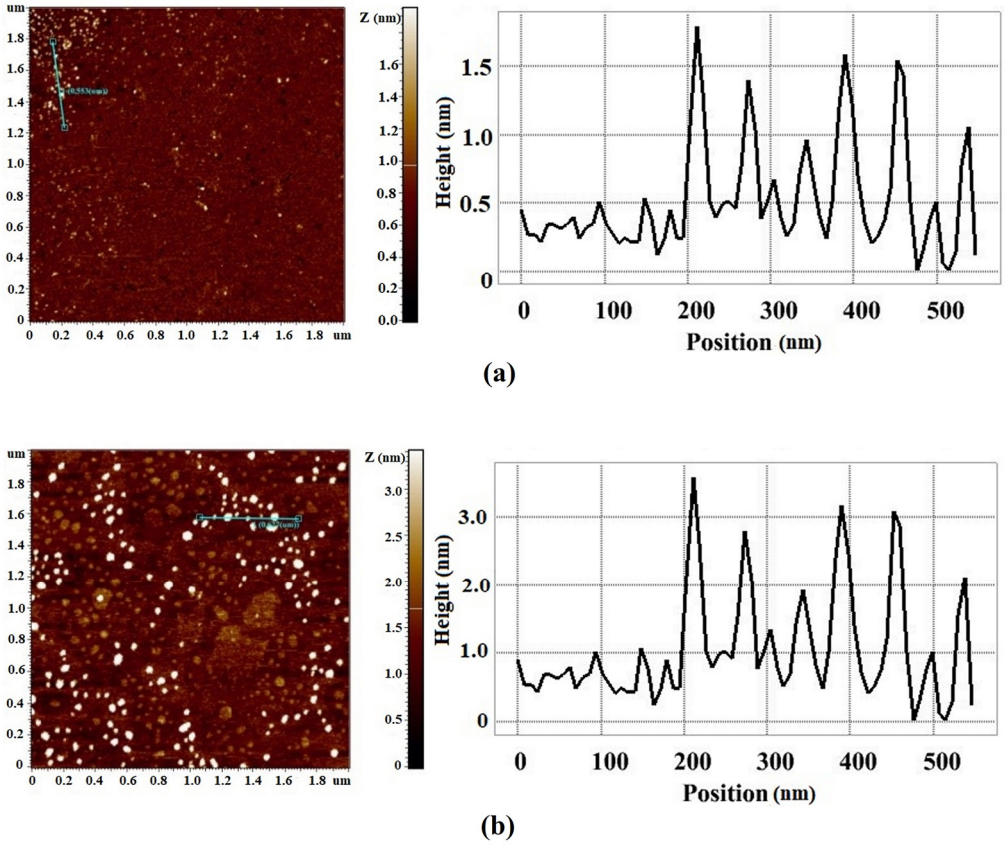

Figure 2. Results of atomic force microscopy (AFM) analysis for horseradish peroxidase (HRP) solutions: typical AFM images of the mica surface with adsorbed HRP particles (left) and corresponding cross-section profiles indicated by lines in the AFM images (right). The measuring cell

(containing HRP solution) was placed either far away at a 10-m distance from the polymeric pipe coil (control experiment) (**a**) or over the coil (**b**).

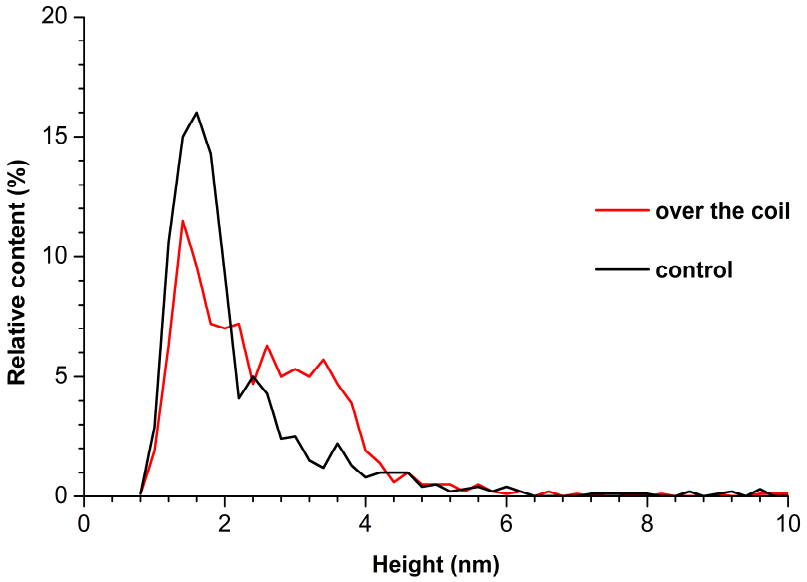

Figure 3. Results of processing of data obtained upon the AFM analysis of HRP solutions. Typical plots of distribution of the imaged objects with height $\rho(h)$. The cell with HRP solution was placed either far away at a 10-m distance from the polymeric pipe coil (control experiment, black line) or over the coil (red line).

At the same time, the $\rho(h)$ plot for the control sample has an inflection point near 2.2 nm, which indicates a non-monotonic dip of the $\rho(h)$ curve near this point. The latter indicates that there is an additional contribution from objects with high heights (i.e., aggregates of biomolecules) to the right wing of the distribution in the region of heights above 2.2 nm. That is, it has been observed that HRP biomolecules, adsorbed from the control solution, present on the AFM chip in the form of a mixture of monomers and aggregates.

Figure 2b displays typical AFM images of the mica surface with HRP biomolecules adsorbed from the solution placed in the cell over the coil (see Figure 1). As seen from Figure 2b, objects with heights from 1 to 5 nm are visualized. The analysis of $\rho(h)$ function obtained for this sample (Figure 3, red line) indicated that the distribution maximum is 1.4 ± 0.2 nm, what coincides with analogous values obtained for the other sample. However, a significant increase in the contribution to the right wing of the distribution—that is, an increased number of objects with heights from 2.2 to 4.2 nm—is observed. The appearance of objects with heights in the range from 2 to 4 nm on the mica surface after its incubation in the analyzed sample indicates an increase in the protein aggregation rate in the analyzed solution.

3.2. Results of Spectrophotometric Measurements

Measurements of enzymatic activity of HRP using the reaction with ABTS substrate were carried out for all the samples (control and working), as described in Materials and Methods. Typical time dependencies of light absorbance at 405 nm are shown in Figure 4. From this figure, it is clearly seen that virtually no change in the enzymatic activity of HRP is observed for all the solutions tested.

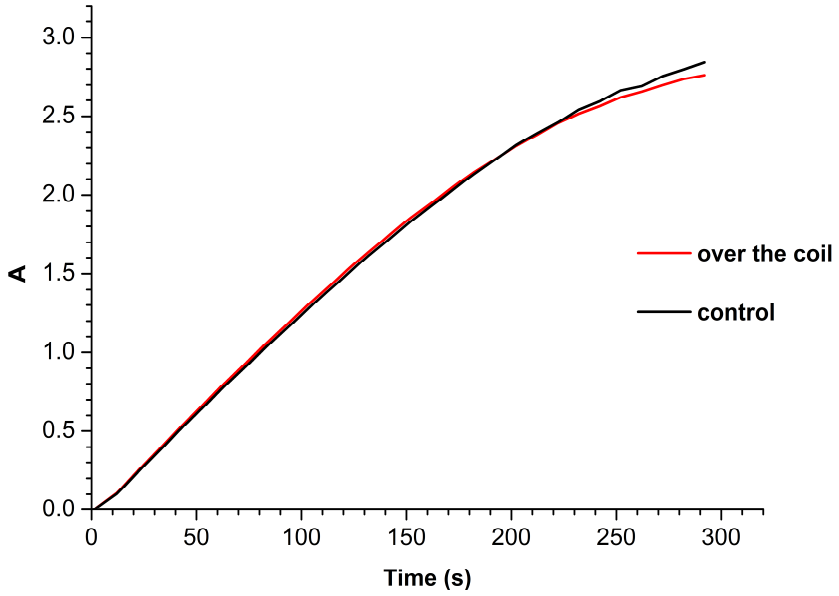

Figure 4. Spectrophotometric measurements of enzymatic activity of HRP. Characteristic time dependencies of change in solution absorbance at 405 nm obtained for control HRP sample and for HRP samples incubated in the experimental setup. The measuring cell (containing HRP solution) was placed either far away at a 10-m distance from the polymeric pipe coil (control experiment; black line) or over the coil (red line). Experimental conditions: HRP:ABTS:H_2O_2 = 10^{-9} M:3 mM:2.5 mM. T = 23 °C.

3.3. Monitoring of the Effect of an Inductive Field on Macroscopic Objects

It has been found that an inductive field, arising from the motion of water, can act on a metallic disc, causing its mechanical movement. That is, after starting the water flow through the polymeric pipe coil, a rotation of this disc, which was placed into the glass cylinder (see Figure 1), was observed. In our experiments, a rotation of the disc by 520 degrees anti-clockwise for about 7 min was observed, followed by a 225-degree rotation in the opposite direction for 15 min; after that, the disc exhibited minor movements during the rest of the observation time. The complete video record of the full experiment after starting the water flow can be found in the Supplementary movie files (two versions of the movie—either a real-time record and a 100X-accelerated video—are provided).

4. Discussion

In the present research, we have studied the effect of water motion through a polymeric pipe. The results obtained indicate the effect of the water flow on a protein solution placed along the axis of a coiled communication. In this way, according to the results of our experiments, through the AFM analysis of the solution placed along the axis of the polymeric communication pipe upon the flow of water through this pipe, formation of large objects with heights from 2 to 4 nm (Figure 3, red line) is observed. This increase in the heights of the AFM-visualized objects corresponds to an increase in protein aggregation.

The cause of the effect of the flow on protein aggregation is possibly connected with the arising of an inductive field upon the motion of water through the pipe—for instance, due to a generation of charge in the moving liquid [5,11,12] and, accordingly, induction of an electromagnetic field. It is interesting to emphasize that, while the change in protein aggregation is clearly observed with the AFM sensor, the enzymatic activity measured by spectrophotometry remains virtually unchanged. The latter means that this influence impacts the spatial structures of the protein, while not affecting its active site. Let us note that the effects of HRP aggregation in the presence of alternating magnetic fields were previously observed by Sun et al. [25]. In our case, alternating magnetic field arises in the

moment of starting the liquid flow, which causes a change in the current generated upon the motion of liquid owing to triboelectric effect; the latter was discussed earlier by us and by other authors [2–6,11–13,38]. It should be emphasized that herein, we have studied the effect of a flow of tap water through a coiled polymeric communication pipe. According to the results reported by Xu et al. [11] and by Zhao et al. [12], despite the resistivity of tap water being much lower than that of a purified (distilled of deionized) one, its flow along a polymeric surface is expected to produce a considerable triboelectric effect. As was noted in the introduction, Xu et al. observed a considerable triboelectric effect caused by the falling of liquid drops onto a poly(tetrafluoroethylene) (PTFE) surface. The ionic strength of tap water used by Xu et al. was 3.1 mM, which is of the same order of magnitude as the water employed in our experiments. Let us note that the triboelectric effect observed by Xu et al. upon dropping tap water onto PTFE allowed the authors to attain a 50 W/m^2 output power; at that, a ~140 V voltage was generated. This was sufficient to power 100 LEDs. The authors also demonstrated that such a system is even capable of producing electric power when using seawater, allowing them to generate a ~20 V voltage.

As regards our study, we observed the influence of a triboelectric effect of moving tap water not in a drop-by-drop, but in a more efficient jet flow mode with a 4 m/s flow speed.

Let us note that the intensity of the inductive field, arising upon the motion of liquid, is sufficiently high, an example of the effect of which could be observed in the rotation of a disc, hung on a cobweb thread inside a cylinder with a spiral-wound communication pipe with flowing water. Such a behaviour is possibly caused by an interference between the inductive fields arising upon the flow of water through the polymeric pipe and those arising on the metal disc. The intensity of these fields is significant, the effect of which manifests itself in mechanical rotation of the disc.

The results obtained indicate the effect of water flowing through polymeric communications on an enzyme located near these communications. These results should be taken into account in the development of models describing the physicochemical properties of proteins (including their aggregation state) and in biosensor systems. This is particularly important to be taken into account in highly sensitive biosensors for diagnostics of oncological diseases, such as brain cancer, prostate cancer, breast cancer, ovarian cancer. These results are also of importance for modeling pathological processes connected with the participation of enzymes in the formation of functionally important multiprotein complexes—for instance, inflammatory processes in the body with the participation of myeloperoxidase, which is present in the form of dimers in these complexes [39]. Evidently, if peroxidase changes its aggregation state under the influence of an electric field, then the influence of radiation on the course of inflammation-associated pathological process is also possible. Moreover, protein aggregation can lead to hemodynamic difficulties in small vessels.

5. Conclusions

Herein, with the example of HRP protein, studied with an AFM sensor, it has been shown that a water flow, formed in the flow sections of biosensors, has an effect on the enzyme—namely, the change in its aggregation state has been observed. It has been demonstrated that the flow of water through a coiled polymeric communication pipe impacts the physicochemical properties of the protein. This effect manifests itself in the form of an increase in the degree of HRP aggregation upon its adsorption onto the bare muscovite mica surface. This indicates that water, flowing through the coiled pipe, influences the spatial structures of the protein. At the same time, no influence of the water flow on the functional activity of the protein was registered, as its enzymatic activity, estimated by conventional spectrophotometry, remained unchanged. The results reported herein are of importance for the correct interpretation of data obtained during the studies involving proteins (including enzymes) in flow-based biosensor systems. These results should be taken into account in the development of models describing protein aggregation and hemodynamics. Our results are also important for the development of novel highly sensitive biosensors intended for the diagnosis of diseases connected with protein aggregation—in particular, inflammatory processes, neurodegenerative diseases, and oncological diseases.

Supplementary Materials: The following are available online at www.mdpi.com/2076-3417/10/13/4560/s1, Video S1: a real-time record; Video S2: 100X-accelerated video.

Author Contributions: Y.D.I., T.O.P. and V.Y.T. conceived and designed the experiments; T.O.P., I.D.S., A.F.K., A.A.V. and V.S.Z. performed the experiments; A.F.K., T.S.R., A.A.V. and I.N.S. analyzed data; V.Y.T. and I.N.S. provided materials and resources; Y.D.I., T.O.P. and I.D.S. wrote the paper. All authors have read and agreed to the published version of the manuscript.

Funding: The work was performed in the framework of the Program for Basic Research of State Academies of Sciences for 2013-2020.

Conflicts of Interest: the authors declare no conflict of interest.

Data Availability: The datasets generated during and/or analyzed during the current study are available from the corresponding author on reasonable request.

References

1. Doran, P.M. Heat transfer. In *Bioprocess Engineering Principles*, 2nd ed.; Doran, P.M., Ed.; Elsevier: Oxford, UK, 2013; pp. 333–377.
2. Choi, D.; Lee, H.; Im, D.J.; Kang, I.S.; Lim, G.; Kim, D.S.; Kang, K.H. Spontaneous electrical charging of droplets by conventional pipetting. *Sci. Rep.* **2013**, *3*, 1–7, doi:10.1038/srep02037.
3. Ivanov, Y.D.; Kozlov, A.F.; Galiullin, R.A.; Ivanova, N.D.; Tatur, V.Y.; Ziborov, V.S.; Yushkov, E.S.; Pleshakova, T.O. Generation and accumulation of charge in a flow system for detecting protein markers of diseases. *Pathol. Physiol. Exp. Ther. Rus. J.* **2017**, *61*, 167–175.
4. Stetten, A.Z.; Golovko, D.S.; Weber, S.A.L.; Butt, H.-J. Slide electrification: charging of surfaces by moving water drops. *Soft Matter* **2019,** *15*, 8667–8679, doi:10.1039/C9SM01348B.
5. Burgo, T.A.L.; Galembeck, F.; Pollack, G.H. Where is water in the triboelectric series? *J. Electrost.* **2016,** *80*, 30–33, doi:10.1016/j.elstat.2016.01.002.
6. Ivanov, Y.D.; Kozlov, A.F.; Galiullin, R.A.; Tatur, V.Y.; Ivanova, N.D.; Ziborov, V.S. Influence of chip materials on charge generation in flowing solution in nanobiosensors. *Appl. Sci.* **2019**, *9*, 671, doi:10.3390/app9040671.
7. Zinoviev, S.V. Nonlinear interactions of weak electromagnetic radiation with biological objects: Physical mechanisms. In *Intellectual Forum—Open the Door*; NII PMM: Saint-Petersburg, Russia, 2007; pp. 33–38.
8. Golovin, Y.I.; Klyachko, N.L.; Majouga, A.G.; Gribanovskii, S.L.; Golovin, D.Y.; Zhigachev, A.O.; Shuklinov, A.V.; Efremova, M.V.; Veselov, M.M.; Vlasova, K.Y.; et al. New approaches to nanotheranostics: multifunctional magnetic nanoparticles activated by a non-warming low-frequency magnetic field control a biochemical system with molecular locality and selectivity. *Russ. Nanotechnol.* **2018**, *13*, 3–25, doi:10.1134/S1995078018030060.
9. Trecazzi, C.; Fisher, M.T. Detecting protein pre-aggregation states using chaperonin biosensor bio-layer interferometry. *Am. Pharm. Rev.* **2018**, *21*, 52–55.
10. Pace, S.E.; Joshi, S.B.; Esfandiary, R.; Stadelman, R.; Bishop, S.L.; Middaugh, C.R.; Fisher, M.T.; Volkin, D.B. The use of a GroEL-BLI biosensor to rapidly assess preaggregate populations for antibody solutions exhibiting different stability profiles. *J. Pharm. Sci.* **2018**, *107*, 559–570, doi:10.1016/j.xphs.2017.10.010.
11. Xu, W.; Zheng, H.; Liu, Y.; Zhou, X.; Zhang, C.; Song, Y.; Xu, D.; Leung, M.; Yang, Z.; Xu, R.X.; et al. A droplet-based electricity generator with high instantaneous power density. *Nature* **2020**, *578*, 392–396, doi:10.1038/s41586-020-1985-6.
12. Zhao, L.; Liu, L.; Yang, X.; Hong, H.; Yang, Q.; Wang, J.; Tang, Q. Cumulative charging behavior of water droplets driven freestanding triboelectric nanogenerator toward hydrodynamic energy harvesting. *J. Mater. Chem. A* **2020**, *8*, 7880–7888, doi:10.1039/D0TA01698E.
13. Haque, R.I.; Arafat, A.; Briand, D. Triboelectric effect to harness fluid flow energy. *J. Phys.: Conf. Ser.* **2019**, *1407*, 012084, doi:10.1088/1742-6596/1407/1/012084.
14. Veitch, N.C. Horseradish peroxidase: a modern view of a classic enzyme. *Phytochemistry* **2004**, *65*, 249–259, doi:10.1016/j.phytochem.2003.10.022.
15. Vlasova, I.I. Peroxidase activity of human hemoproteins: keeping the fire under control. *Molecules* **2018**, *23*, 2561, doi:10.3390/molecules23102561.

16. Tao, Z.; Zhou, Y.; Li, X.; Wang, Z. Competitive HRP-linked colorimetric aptasensor for the detection of fumonisin B1 in food based on dual biotin-streptavidin interaction. *Biosensors* **2020**, *10*, 31, doi:10.3390/bios10040031.
17. Guo, W.-J.; Yang, X.-Y.; Wu, Z.; Zhang, Z.-L. A colorimetric and electrochemical dual-mode biosensor for thrombin using a magnetic separation technique. *J. Mater. Chem. B* **2020**, *8*, 3574–3581, doi:10.1039/c9tb02170a.
18. Metzler, D.E. *Biochemistry: The Chemical Reactions of Living Cells*; Academic Press: Oxford, UK, 1970.
19. Rogozhin, V.V.; Kutuzova, G.D.; Ugarova, N.N. Inhibition of horseradish peroxidase by N-ethylamide of o-sulfobenzoylacetic acid. *Bioorganic Chem.* **2000**, *26*, 156–160.
20. Gavrilenko, T.I.; Ryzhkova, N.A.; Parkhomenko, A.N. Myeloperoxidase and its role in the development of coronary heart disease. *Ukr. J. Cardiol.* **2014**, *4*, 119–126.
21. Davies, P.F.; Rennke, H.G.; Cotran, R.S. Influence of molecular charge upon the endocytosis and intracellular fate of peroxidase activity in cultured arterial endothelium. *J. Cell Sci.* **1981**, *49*, 69–86.
22. Welinder, K.G. Amino acid sequence studies of horseradish peroxidase: Amino and carboxyl termini, cyanogen bromide and tryptic fragments, the complete sequence, and some structural characteristics of horseradish peroxidase C. *Eur. J. Biochem.* **1979**, *96*, 483–502, doi:10.1111/j.1432-1033.1979.tb13061.x.
23. Ignatenko, O.V.; Sjölander, A.; Hushpulian, D.M.; Kazakov, S.V.; Ouporov, I.V.; Chubar, T.A.; Poloznikov, A.A.; Ruzgas, T.; Tishkov, V.I.; Gorton, L.; et al. Electrochemistry of chemically trapped dimeric and monomeric recombinant horseradish peroxidase. *Adv. Biosens. Bioelectron.* **2013**, *2*, 25–34.
24. Sun, J.; Sun, F.; Xu, B.; Gu, N. The quasi-one-dimensional assembly of horseradish peroxidase molecules in presence of the alternating magnetic field. *Coll. Surf.* A *Physicochem. Eng. Aspects* **2010**, *360*, 94–98, doi:10.1016/j.colsurfa.2010.02.012.
25. Sun, J.; Zhou, H.; Jin, Y.; Wang, M.; Gu, N. Magnetically enhanced dielectrophoretic assembly of horseradish peroxidase molecules: chaining and molecular monolayers. *Chem. Phys. Chem.* **2008**, *9*, 1847–1850, doi:10.1002/cphc.200800237.
26. Ivanov, Y.D.; Pleshakova, T.O.; Shumov, I.D.; Kozlov, A.F.; Ivanova, I.A.; Valueva, A.A.; Tatur, V.Y.; Smelov, M.V.; Ivanova, N.D.; Ziborov, V.S. AFM imaging of protein aggregation in studying the impact of knotted electromagnetic field on a peroxidase. *Sci. Rep.* **2020**, *10*, 9022, doi:10.1038/s41598-020-65888-z.
27. Ivanov, Y.D.; Bukharina, N.S.; Frantsuzov, P.A.; Pleshakova, T.O.; Kanashenko, S.L.; Medvedeva, N.V.; Argentova, V.V.; Zgoda, V.G.; Munro, A.W.; Archakov, A.I. AFM study of cytochrome CYP102A1 oligomeric state. *Soft Matter* **2012**, *8*, 4602–4608, doi:10.1039/C2SM07333A.
28. Ivanov, Y.D.; Danichev, V.V.; Pleshakova, T.O.; Shumov, I.D.; Ziborov, V.S.; Krokhin, N.V.; Zagumenniy, M.N.; Ustinov, V.S.; Smirnov, L.P.; Archakov, A.I. Irreversible chemical AFM-based fishing for the detection of low-copied proteins. *Biochem. Suppl. Ser. B Biomed. Chem.* **2013**, *7*, 46–61, doi:10.1134/S1990750813010071.
29. Dufrêne, Y.F.; Ando, T.; Garcia, R.; Alsteens, D.; Martinez-Martin, D.; Engel, A.; Gerber, C.; Müller, D.J. Imaging modes of atomic force microscopy for application in molecular and cell biology. *Nature Nanotechnol.* **2017**, *12*, 295–307, doi:10.1038/nnano.2017.45.
30. Pleshakova, T.O.; Bukharina, N.S.; Archakov, A.I.; Ivanov, Y.D. Atomic force microscopy for protein detection and their physicochemical characterization. *Int. J. Mol. Sci.* **2018**, *19*, 1142, doi:10.3390/ijms19041142.
31. Kiselyova, O.I.; Yaminsky, I.V.; Ivanov, Y.D.; Kanaeva, I.P.; Kuznetsov, V.Y.; Archakov, A.I. AFM study of membrane proteins, cytochrome P450 2B4, and NADPH-Cytochrome P450 reductase and their complex formation. *Arch. Biochem. Biophys.* **1999**, *371*, 1–7, doi: 10.1006/abbi.1999.1412
32. Pleshakova, T.O.; Kaysheva, A.L.; Shumov, I.D.; Ziborov, V.S.; Bayzyanova, J.M.; Konev, V.A.; Uchaikin, V.F.; Archakov, A.I.; Ivanov, Y.D. Detection of hepatitis C virus core protein in serum using aptamer-functionalized AFM chips. *Micromachines* **2019**, *10*, 129, doi:10.3390/mi10020129.
33. Sanders, S.A.; Bray, R.C.; Smith, A.T. pH-dependent properties of a mutant horseradish peroxidase isoenzyme C in which Arg38 has been replaced with lysine. *Eur. J. Biochem.* **1994**, *224*, 1029–1037, doi:10.1111/j.1432-1033.1994.01029.x.
34. Enzymatic Assay of Peroxidase (EC 1.11.1.7) 2,2′-azino-bis(3-ethylbenzthiazoline-6-sulfonic acid) as a Substrate Sigma Prod. No. P-6782. Available online: https://www.sigmaaldrich.com/content/dam/sigma-aldrich/docs/Sigma/Enzyme_Assay/p6782enz.pdf (accessed on 16 June 2020).

35. Unger, B.P.; Gunsalus, I.C.; Sligar, S.G. Nucleotide sequence of the Pseudomonas putida cytochrome P-450cam gene and its expression in Escherichia coli. *J. Biol. Chem.* **1986**, *261*, 1158–1163.
36. Ivanov, Y.D.; Frantsuzov, P.A.; Zöllner, A.; Medvedeva, N.V.; Archakov, A.I.; Reinle, W.; Bernhardt, R. Atomic force microscopy study of protein-protein interactions in the cytochrome CYP11A1 (P450scc)-containing steroid hydroxylase system. *Nanoscale Res. Lett.* **2011**, *6*, 1–13, doi:10.1007/s11671-010-9809-5.
37. Chu, J.-W.; Kimura, T. Studies on adrenal steroid hydroxylases Molecular and catalytic properties of adrenodoxin reductase (a flavoprotein). *J. Biol. Chem.* **1973**, *248*, 2089–2094.
38. Ivanov, Y.D.; Kozlov, A.F.; Galiullin, R.A.; Tatur, V.Y.; Ziborov, V.S.; Usanov, S.A.; Pleshakova, T.O. Influence of a pulsed electric field on charge generation in a flowing protein solution. *Separations* **2018**, *5*, 29, doi:10.3390/separations5020029.
39. Samygina, V.R.; Sokolov, A.V.; Bourenkov, G.; Petoukhov, M.V.; Pulina, M.O.; Zakharova, E.T.; Vasilyev, V.B.; Bartunik, H.; Svergun, D.I. Ceruloplasmin: macromolecular assemblies with iron-containing acute phase proteins. *PLoS One* **2013**, *8*, e67145, doi:10.1371/journal.pone.0067145.